JB
Journals.ASM.org

SalB Inactivation Modulates Culture Supernatant Exoproteins and Affects Autolysis and Viability in *Enterococcus faecalis* OG1RF

Jayendra Shankar, Rachel G. Walker,* Mark C. Wilkinson, Deborah Ward, and Malcolm J. Horsburgh

Institute of Integrative Biology, University of Liverpool, Liverpool, United Kingdom

The culture supernatant fraction of an *Enterococcus faecalis gelE* mutant of strain OG1RF contained elevated levels of the secreted antigen SalB. Using differential fluorescence gel electrophoresis (DIGE) the *salB* mutant was shown to possess a unique complement of exoproteins. Differentially abundant exoproteins were identified using matrix-assisted laser desorption ionization–time of flight (MALDI-TOF) mass spectrometry. Stress-related proteins including DnaK, Dps family protein, SOD, and NADH peroxidase were present in greater quantity in the OG1RF *salB* mutant culture supernatant. Moreover, several proteins involved in cell wall synthesis and cell division, including D-Ala-D-Lac ligase and EzrA, were present in reduced quantity in OG1RF *salB* relative to the parent strain. The *salB* mutant displayed reduced viability and anomalous cell division, and these phenotypes were exacerbated in a *gelE salB* double mutant. An epistatic relationship between *gelE* and *salB* was not identified with respect to increased autolysis and cell morphological changes observed in the *salB* mutant. SalB was purified as a six-histidine-tagged protein to investigate peptidoglycan hydrolytic activity; however, activity was not evident. High-pressure liquid chromatography (HPLC) analysis of reduced muropeptides from peptidoglycan digested with mutanolysin revealed that the *salB* mutant and OG1RF were indistinguishable.

Enterococci are commensals of the animal gut, and several species cause disease in humans, including wound and urinary tract infections, endocarditis, and bacteremia. *Enterococcus faecalis* and *Enterococcus faecium* have become increasingly problematic due to rising rates of infection, combined with accumulated resistance to antibiotics (4, 27). *E. faecalis* is the most virulent species in the genus and the cause of approximately 80% of all enterococcal infections, with virulence factors that include adhesins, proteases, and cytolysin (10, 11, 33). The accumulation of resistance genes is important medically, since intergeneric horizontal transfer of antibiotic resistance genes involving *Staphylococcus aureus* and *Listeria* species has been reported (3, 16, 20, 30, 38).

E. faecalis strains with an intact Fsr quorum sensing system temporally express metalloprotease (GelE) and serine protease (SprE) (19), and these are the two most abundant exoproteins in post-exponential-growth-phase cultures (21, 29). GelE, a member of the peptidase M4 family, proteolytically activates the major cell wall *N*-acetylglucosaminidase, AtlA (35), which contributes to cell separation after cell division (1, 15). The *E. faecalis* exoprotein SalB is a paralogue of the essential *E. faecium* cell wall-associated SagA (34) and streptococcal PcsB proteins (23, 24). The enzymatic activity of these proteins has not been unambiguously determined, but bioinformatic analysis supports peptidoglycan hydrolase activity and PcsB was reported to interact with the essential cell division protein, FtsX (28). The genes encoding SalA/SagA/PcsB have a conserved location in each species downstream of genes encoding the cell shape-determining proteins MreC and MreD (13, 23). *E. faecalis* SalB shares ~40% primary amino acid sequence identity (~70% similarity) with streptococcal PcsB.

E. faecalis SalB is not essential for growth. Inactivation of *salB* increased the capability of the bacterium to bind the extracellular matrix (ECM) molecules fibronectin and collagen type I and enhanced biofilm production when grown with serum, relative to the wild type (17). A lack of SalB activity results in reduced resistance to a range of stressors, including bile salts, detergent, ethanol, peroxide, heat, and low pH (25). Morphological changes including septation anomalies and increased numbers of spherical cells were identified in a *salB* mutant of *E. faecalis* strain JH2-2, and the mutant had a growth defect in complex medium relative to its isogenic parent (5). SalB expression is induced by extracellular stress via the two-component signal transduction system CroRS in strain JH2-2 (18).

In this study, SalB was found at elevated levels in the culture supernatant of strain TX5264 (OG1RF *gelE*). To investigate a potential epistatic relationship between GelE and SalB, double mutant strains Liv1016 (OG1RF *gelE salB*) and Liv1013 (OG1RF *fsrB salB*) were constructed and compared with strain Liv729 (OG1RF *salB*) and the wild-type parent OG1RF strain. Strain Liv729 (OG1RF *salB*) expresses a distinct set of exoproteins compared with its isogenic parent, potentially indicating a cellular role for SalB.

MATERIALS AND METHODS

Strains and culture conditions. *E. faecalis* strains were routinely cultured in brain heart infusion (BHI) broth (Lab M) or BHI solidified with 1.5% (wt/vol) agar (Table 1). *Escherichia coli* strains were cultured using Luria-Bertani (LB) medium. Antibiotics were added at selective concentrations for the maintenance of plasmids, prior to comparative analyses (Table 1). Culture conditions for *E. faecalis* were 50 ml BHI in a 250-ml conical flask incubated with shaking at 37°C and with growth monitored at 600 nm.

Received 9 March 2012 Accepted 28 April 2012

Published ahead of print 4 May 2012

Address correspondence to Malcolm J. Horsburgh, M.J.Horsburgh@liverpool.ac.uk.

* Present address: Rachel G. Walker, Society for General Microbiology, Spencers Wood, Reading, United Kingdom.

doi:10.1128/JB.00376-12

TABLE 1 Strains and plasmids used in this study

Bacterium strain or plasmid	Strain ID	Characteristics	Marker	Source
E. faecalis strains				
OG1RF	TX4002	Wild type, Rif^r/Fus^r		7
JH2-2		Wild type, Rif^r/Fus^r		12
OG1RF *gelE*	TX5264	In-frame deletion of *gelE*		27
OG1RF *fsrB*	TX5266	*fsrB* mutant		18
OG1RF *fsrB* pTEX5249	Liv305	*fsrB* mutant complemented with *fsrABDC*	Erm	27
OG1RF *salB*	Liv729	*salB* insertional inactivation using pTEX4577	Kan	This study
OG1RF *salB* pAT18::*salB*	Liv883	Complemented *salB* mutant	Kan, Erm	This study
JH2-2 *salB*	Liv1012	*salB* insertional inactivation using pTEX4577	Kan	This study
OG1RF *fsrB salB*	Liv1013	*salB* inactivation in OG1RF *fsrB* background	Kan	This study
OG1RF *gelE salB*	Liv1016	*salB* inactivation in OG1RF *gelE* background	Kan	This study
E. coli strains				
BL21(DE3) pLysS		F^- *ompT* $hsdS_B(r_B^- m_B^-)$ *gal dcm* (DE3)	Cm	30
TOP10		Cloning host		Invitrogen
BL21(DE3) pLysS pJAY1		SalB expression strain	Kan, Cm	This study
Plasmids				
pTEX4577		Insertional inactivation plasmid	Kan	33
pAT18		Shuttle vector	Erm	28
pET24d (+)		T7 RNA polymerase vector His-tag	Kan	Novagen
pRGW1		pTEX4577 with 587-bp *salB* fragment	Kan	This study
pJAY1		pET24d+ with 1,265-bp fragment of *salB*	Kan	This study
pJAY2		pAT18 with 1,645-bp *salB* operon	Erm	This study

Molecular cloning. For insertional inactivation of the *salB* gene, a 587-bp internal gene fragment was amplified by PCR from the chromosome of *E. faecalis* OG1RF using primers SalBKO_BamHI (5′-AAGGATCCTCTAAGCCAGCTTTAGAAC) and SalBKO_EcoRI (5′-CCGAATTCCGCTATCAGCAATTGCTAC) (where underlining indicates the restriction enzyme sequence), digested with BamHI/EcoRI, and ligated (11) to digested suicide plasmid pTEX4577 (36) to create pRGW1. The latter plasmid was used to transform OG1RF, TX5264 (OG1RF *gelE*), and TX5266 (OG1RF *fsrB*) to create the isogenic mutants Liv729 (OG1RF *salB*), Liv1016 (OG1RF *gelE salB*), and Liv1013 (OG1RF *fsrB salB*). A *salB* complementation plasmid was made by ligating the BamHI/EcoRI-digested 1,645-bp *salB* operon of *E. faecalis* OG1RF, which was amplified by PCR using primers SalBcBamHI (5′-CCACGGATCCGTGAAAACCAGTCGTGAC) and SalBcEcoRI (5′-ACATGAATTCTTAGAATACCACGTTTAGC) to digested plasmid pAT18 (31), producing pJAY2. Strain Liv729 (OG1RF *salB*) was transformed to create strain Liv883 (OG1RF *salB* pAT18::*salB*).

To obtain the six-histidine-tagged enzyme, the *salB* gene was amplified and digested to produce a 1,265-bp NcoI/XhoI product using primers SalBOexF (5′-GTACCCATGGACAATGTTGATAAAAAA) and SalBOexR (5′-GTACCTCGAGGGCTGAGTGTCCTACGATTG). This product was ligated to digested pET24d+ (Novagen) to create plasmid pJAY1. The fidelity of the cloned *salB* gene was confirmed by DNA sequencing (GATC Biotech). The six-histidine-tagged SalB was expressed in strain *E. coli* BL21 (λDE3) pLysS following induction of log-phase cells in LB containing 0.5 M glucose with 1 mM IPTG (isopropyl-β-D-thiogalactopyranoside). Cells were lysed using sonication, and the protein was purified under native conditions using Probond chelate resin (Invitrogen) according to the manufacturer's instructions.

Exoprotein analysis. Separation of proteins using one-dimensional (1D) SDS-PAGE was performed after precipitation of cell culture supernatant proteins with 10% (wt/vol) trichloroacetic acid (TCA). Exoprotein purification for 2D SDS-PAGE used a previously described method (6). Exoproteins (500 μg) were focused using a pH 4 to 7 strip (Bio-Rad) and then separated in the second dimension using a 12% (wt/vol), 20 cm by 20 cm polyacrylamide gel. Gels were stained using colloidal Coomassie, scanned using a Gel Imager, and analyzed by using SameSpots software (Progenesis). For comparative proteomics of strains OG1RF and Liv729 (OG1RF *salB*), 80 μg exoprotein from each was labeled with the Cy dyes (GE Healthcare) Cy3 and Cy5, respectively, according to the manufacturer's instructions, before focusing and separation as for the 2D SDS-PAGE protocol. Dye swap controls were performed to confirm labeling efficiency. As an internal control, 40 μg exoprotein from each strain was pooled and stained with Cy2 dye and separated with the samples. Gel images were captured using a Typhoon gel imager and compiled using Adobe Photoshop software. The cutoff criteria for differential quantification (1.5-fold) were used based upon the manufacturer's literature.

Protein spots of interest were excised from the gels and digested overnight with digest buffer containing Trypsin Gold (20 ng μl^{-1}), mass spectrometry (MS) grade (Promega). The peptide mass fingerprints were derived by matrix-assisted laser desorption ionization–time of flight (MALDI-TOF) analysis of tryptic fragments using a Voyager DE Pro (Applied Biosystems). Mass lists were transferred to the Mascot peptide mass fingerprint database (Matrix Science, Ltd.), where they were used to search for matches within the *Firmicutes*. A peptide tolerance of ±0.5 Da and up to one missed peptide cleavage was allowed. Fixed carboxymethyl modifications and variable oxidation modifications were allowed.

Peptidoglycan hydrolase zymograms. Peptidoglycan hydrolase activity was visualized after proteins were separated by SDS-PAGE, supplementing the resolving gel with 10 optical density at 600 nm (OD_{600}) units of purified peptidoglycan isolated from the cell walls of *E. faecalis* or *Micrococcus luteus* (26, 32). After separation, gels were washed for 30 min in distilled water and then renaturing buffer (10 mM $MgCl_2$, 25 mM Tris-HCl, 10% [vol/vol] Triton X-100). Gels were incubated overnight at 37°C in fresh renaturing buffer and then washed with distilled water prior to staining (0.05% [wt/vol] methylene blue in 1 mM KOH) for 2 h. The gel was destained and then repeatedly washed with distilled water until bands of clearing appeared.

Autolysis assay. Exponential-phase cells were harvested and washed with phosphate-buffered saline (PBS) prior to their resuspension in PBS containing either 0.1% (vol/vol) Triton X-100 or 0.1 mg ml^{-1} penicillin G

and incubated at 37°C with shaking. Lysis was monitored by measuring OD_{600}.

Imaging and viability staining. An equal volume of exponential-growth-phase bacterial culture and freshly prepared Live/Dead BacLight (Invitrogen) stain (6 μM Syto9 and 30 μM propidium iodide [PI]) was incubated at room temperature for 15 min in the dark. Ten microliters stained cells was mounted between two coverslips and visualized using a Carl Zeiss LSM 710 laser scanning microscope equipped with dual-emission filters for visualizing Syto9- and PI-stained cells simultaneously. Mean green and red fluorescence levels of Live/Dead Baclight-stained cells from 100,000 events were measured using a flow cytometer. The total fluorescence was gated, and propidium iodide-stained dead cells were plotted as a percentage of total events in the population for comparison.

For electron microscopy thin sections (40 to 70 μm) of epoxy resin-embedded mid-exponential-phase cells were cut using a Leica microtome and transferred to pioloform-coated grids. The thin sections were then visualized in a 120 kV Technai G2 Spirit Biotwin transmission electron microscope (TEM) with images analyzed by Technai G2 software.

Purification of peptidoglycan and muropeptide analysis. Peptidoglycan was isolated using the procedure of Rosenthal and Dziarski (26). Briefly, cultures of *E. faecalis* OG1RF or *M. luteus* were grown to mid-exponential phase, harvested, washed, and autoclaved. Cells were ruptured five times in a French pressure cell at 14,000 lb/in^2 (>95% breakage). The ruptured cells were harvested at 16,100 relative centrifugal force (RCF) for 5 min and boiled/washed five times in SDTE buffer (2% [wt/vol] SDS, 20 mM dithiothreitol [DTT], 50 mM Tris-HCl, 1 mM EDTA) at 100°C for 10 min and pelleted at 20,000 RCF for 5 min. The final pellet was boiled and washed 6 times in water. The peptidoglycan was isolated by gentle shaking with water between washes. All the peptidoglycan was pooled and harvested by centrifugation at 20,000 RCF for 5 min and resuspended in 1 ml sterile water. Its turbidity was measured at 600 nm, and the sample was stored at −20°C.

The method for the reduction and separation of muropeptides was modified from previous work on *E. faecalis* autolysin AtlA (8). Ten OD units of purified peptidoglycan was incubated at 37°C in 200 mM sodium phosphate buffer at pH 6.0, 0.1 mM $MgCl_2$ with 5 μg mutanolysin (Sigma) or with 45 to 50 μg of SalB to a final volume of 250 μl. Following digestion overnight, the peptidoglycan was centrifuged at 16,000 RCF for 30 min. Supernatant (200 μl) containing soluble muropeptides was recovered and transferred to a fresh Eppendorf tube. An equal volume of 250 mM sodium borate buffer was added with 2 mg of solid sodium borohydride and left at room temperature (RT) for 15 min. Excess sodium borohydride was removed by the addition of 5 μl of *o*-phosphoric acid. Fifty microliters of muropeptides was acidified with 2.5 μl trifluoroacetic acid (TFA) (1% [vol/vol] final concentration) before separation on a Brownlee PepMap C-18 high-pressure liquid chromatography (HPLC) column run on a Beckman-Coulter System Gold HPLC instrument. Muropeptides were separated using a linear gradient of 0 to 45% (vol/vol) acetonitrile in 0.1% (vol/vol) TFA, and elution was monitored at 214 nm.

RESULTS

Inactivation of *gelE* and *salB* alters culture supernatant exoproteins. The contribution made by GelE activity to temporal expression of the exoprotein fraction of *E. faecalis* OG1RF was determined by extracting the culture supernatant proteins of TX5264 (OG1RF *gelE*) after 8 h of growth (determined to be in stationary phase, data not shown) and comparing them to exoproteins from the isogenic parent strain OG1RF (Fig. 1; data not shown). Several novel protein bands were present in the supernatant protein fraction of strain TX5264 (OG1RF *gelE*), including a 55-kDa protein present at all growth stages, which was identified as SalB following trypsin digest and MALDI-TOF mass spectrometry (seven matching peptides; Mowse score = 52). In the culture supernatant of strain OG1RF, there was an absence of SalB from 5 h (mid-exponential growth phase) concomitant with increased protease (GelE and SprE) expression (data not shown). A potential epistatic relationship between *salB* and *gelE* was investigated via insertional inactivation of *salB* in OG1RF and TX5264 (OG1RF *gelE*) to produce strains Liv729 (OG1RF *salB*) and Liv1016 (OG1RF *gelE salB*). Subsequently, since the enzymatic function of SalB remains undetermined in *E. faecalis*, the stationary-phase culture supernatant exoproteins produced by strains Liv729 (OG1RF *salB*) and Liv1016 (OG1RF *gelE salB*) were compared with those of their isogenic parent strains (Fig. 1). A distinct complement of exoproteins was present in the culture supernatant of strain Liv729 (OG1RF *salB*), and this was absent in the complementation strain Liv883 (OG1RF *salB* pAT18::*salB*) (Fig. 1 and data not shown), indicating that the absence of SalB caused changes to the exoproteome. These changes were investigated to determine whether they might reveal a function for SalB.

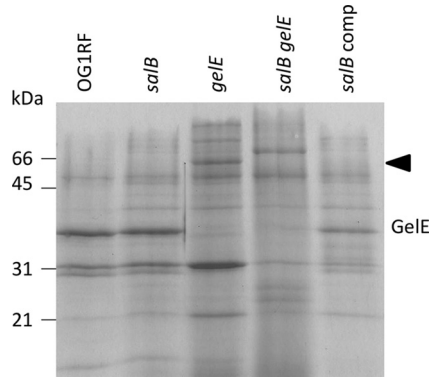

FIG 1 Culture supernatant exoproteins from *E. faecalis* strains. Exoproteins of OG1RF and its isogenic mutants with mutations in *salB* (Liv729 [OG1RF *salB*]), *gelE* (OG1RF *gelE*), *salB gelE* (Liv1016 [OG1RF *salB gelE*]), and *salB* comp (Liv883 [OG1RF *salB* pAT18::*salB*]), harvested at early stationary (8 h) growth phase. Molecular mass markers (kDa) are shown on the left. The arrowhead indicates SalB.

Identification of the *salB* mutant exoproteome. To gain insight into the cellular role of SalB, the exoproteins produced by strain Liv729 (OG1RF *salB*) were quantitatively compared with those of its isogenic parent strain using 2D differential fluorescence gel electrophoresis (DIGE). Based upon a previous exoproteome analysis (29) stationary-phase culture supernatants (stationary phase was determined to be after 8 h of growth; data not shown) were extracted, 80 μg of protein from each strain was separated, and the proteins were compared. The exoprotein fraction from strain Liv729 (OG1RF *salB*) could be distinguished from that of OG1RF largely by the presence of a unique protein set with low pI and high molecular mass (Fig. 2A). Differentially abundant or novel proteins from triplicate gels of strain Liv729 (OG1RF *salB*) were compared using SameSpots software (Progenesis) and quantified relative to OG1RF (Tables 2 and 3). Subsequently, proteins with differential abundance were isolated from a 500-μg exoprotein sample, separated by 2D SDS-PAGE, and oriented relative to the gels from DIGE (Fig. 2A and B). MALDI-TOF mass spectrometry of tryptic digests assigned 24 identities to 31 protein spots that were quantified as being in increased amount in strain Liv729 (OG1RF *salB*) compared with OG1RF, with a fold difference of at least 1.5 (Tables 2 and 3). Thirteen proteins were quantified from OG1RF exoproteome gels (Fig. 2A and data not

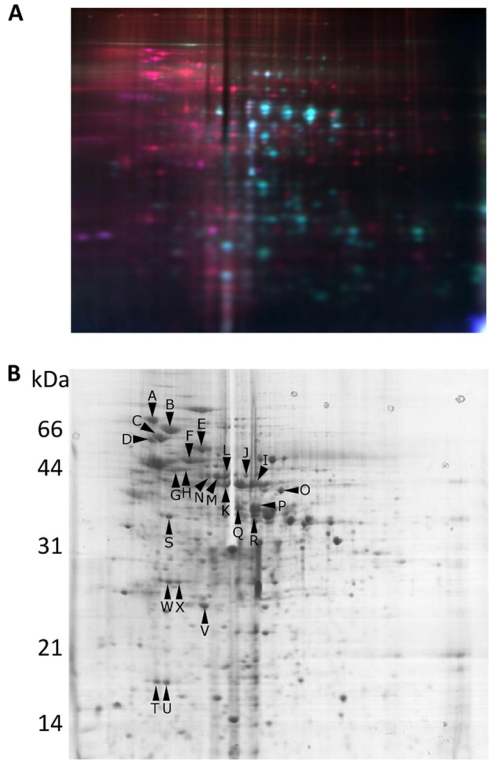

FIG 2 (A) DIGE analysis of culture supernatant exoproteins produced after 8 h of growth by strain Liv729 (OG1RF *salB*), labeled with Cy3 (yellow-green), and those produced by its parent strain OG1RF, labeled with Cy5 (red). (B) Exoproteins produced by strain Liv729 (OG1RF *salB*) and separated by 2D SDS-PAGE, with arrowed letters indicating differentially regulated proteins.

shown) (29) as being decreased or absent in the *salB* mutant strain, with eight spots assigned identities from MALDI-TOF mass spectrometry of tryptic digests (Table 3). Bioinformatic analysis of these identified proteins revealed that many of these have known or proposed roles in the general stress response, cell wall synthesis, cell division, and metabolism.

Effect of *salB* inactivation on cell autolysis. The role of SalB in cell autolysis was explored because of the altered levels of cell wall synthesis and cell division enzymes that were quantified in culture supernatant of the mutant strain; moreover, SalB was hypothesized previously to be a peptidoglycan hydrolase (25). Strain Liv729 (OG1RF *salB*) displayed an increased rate of autolysis compared to the wild type under challenge from either penicillin G (Fig. 3) or Triton X-100 (data not shown). The autolysis phenotype was complemented in Liv883 (OG1RF *salB* pAT18::*salB*) with respect to penicillin G challenge, but only partially for Triton X-100 challenge (data not shown). Inactivation of *gelE* is reported to increase chain length in strain OG1RF and was therefore proposed to have a role in proteolytic activation of autolysins required for daughter cell separation (37). Limited autolysis was confirmed with strain TX5264 (OG1RF *gelE*), when challenged with either penicillin G or Triton X-100. The double mutant strain Liv1016 (OG1RF *gelE salB*) exhibited greater autolysis than did the gelatinase mutant TX5264 (OG1RF *gelE*). These data indicate that the absence of SalB activity increases autolysis in a *gelE* mutant, which supports there being no evidence of epistasis with respect to *salB* and *gelE*, thereby supporting the proteins having opposing roles in autolysis, at least under the conditions studied here.

Cell separation defect and reduced viability of OG1RF *salB* mutant. The observed increase in autolysis and the altered exoprotein expression of strain Liv729 (OG1RF *salB*) support a role for SalB in cell wall homeostasis and/or cell division. Cell separation defects were previously reported to result from *salB* inactivation in strain *E. faecalis* JH2-2, which is naturally GelE negative due to an *fsr* locus deletion (19). A JH2-2 *salB* mutant was reported to have a reduced growth rate under normal culture conditions (5). In contrast, there was no comparable growth rate reduction observed in this study for strain Liv729 (OG1RF *salB*) cultured in BHI (data not shown). Strain Liv1012 (JH2-2 *salB*) was generated in this study by transformation, and the previously described growth rate phenotype was confirmed (data not shown). Thus, *salB* inactivation results in differing phenotypes between host strains OG1RF and JH2-2, the latter of which contains a large deletion encompassing *fsr* (19). Based upon optical density measurements, no growth rate differences were observed during culture of strains Liv1016 (OG1RF *gelE salB*) and Liv1013 (OG1RF *fsrB salB*) (data not shown); consequently, the basis for the growth rate difference in strain Liv1012 (JH2-2 *salB*) remains undetermined.

To study the effect of *salB* inactivation on cell wall synthesis or cell division, the different *salB* mutant strains were investigated by fluorescently labeling nucleic acids. Assay of the cultures using fluorescence-activated cell sorting (FACS) determined that in mid-exponential phase, strain Liv729 (OG1RF *salB*) exhibited a 39-fold relative increase in nonviable cells (propidium iodide, red fluorescence) compared with its isogenic parent strain (Fig. 4; Table 4). The mean green fluorescence (Syto-9) was similar for the two strains, with a 1.8-fold increase for Liv729 (OG1RF *salB*). The effect of *gelE* inactivation was investigated, and cells of strain TX5264 (OG1RF *gelE*) displayed an 8-fold increase in nonviable cells (1.4-fold increase in mean green fluorescence). Moreover, strain Liv1016 (OG1RF *gelE salB*) displayed a 145-fold increase in nonviable cells together with a 5.8-fold increase in mean green fluorescence. A considerable reduction in viability was also observed in strain Liv1013 (OG1RF *fsrB salB*; data not shown). Partial complementation of the viability defect resulting from *salB* inactivation was observed in strain Liv1016 (OG1RF *salB* pAT18::*salB*) (Fig. 4; Table 4).

Laser scanning microscopy of fluorescently stained cells was used to examine cell separation and identified that inactivation of either *gelE* (Fig. 5) or *fsrB* (data not shown) resulted in chains of cells, as previously described (1, 37). In contrast, inactivation of *salB* resulted in cell clumps, which were exacerbated in double mutant strains that had *salB* plus either *gelE* (Fig. 5) or *fsrB* (data not shown) or inactivated. The cell separation phenotypes were confirmed by examining relative sedimentation of exponential cultures. After 30 min of incubation, the strains with the greatest mean green fluorescence and reduced cell separation displayed the greatest level of sedimentation (data not shown). Defective septation of mid-exponential-phase cells of strain Liv729 (OG1RF *salB*) in this study was confirmed by TEM (Fig. 6B) and matched that described for a *salB* mutant of JH2-2 (4, 24). The septation defect was exacerbated in the double mutant strain Liv1016 (OG1RF *gelE salB*) relative to the isogenic single mutant parent strains (Fig. 6A and C).

TABLE 2 Characteristics of proteins extracted in this study

Spot ID	Protein description (accession no.)	Fold change	Calculated mass (kDa)/pI value	No. of peptides matched	Sequence coverage (%)
Group 1, stress-related proteins					
A	DnaK (EF_1308)	2.02	65.54/4.59	12	22
C	GroEL (EF_2633)	4.05	55.41/4.66	13	30
F	NADH peroxidase, Npr (EF_1211)	2.27	49.52/4.83	7	25
T	Dps family protein (EF_3233)	1.85	17.93/4.56	6	47
U	Dps family protein (EF_3233)	3.82	17.93/4.56	5	42
V	Superoxide dismutase (EF_0463)	2.35	15.95/4.96	6	69
Group 2, proteins of metabolic pathways					
B	PEP phosphotransferase enzyme I (EF_0710)	3.03	63.13/4.68	13	21
G	PEP phosphotransferase enzyme I (EF_0710)		63.13/4.68	4	16
E	Dihydrolipoyl dehydrogenase (EF_1356)		49.11/4.95	6	28
I	Glyceraldehyde 3-phosphate dehydrogenase, Gap-2 (EF_1353)	3.35	35.92/5.03	6	38
K	Acetate kinase, AckA (EF_1983)	2.72	43.49/4.96	8	37
L	Phosphoglycerate kinase, Pgk (EF_1963)	2.28	42.37/4.9	8	32
M	Phosphoglycerate kinase (EF_1963)	5.3	42.37/4.9	7	27
N	Phosphoglycerate kinase (EF_1963)	2.39	42.37/4.9	5	17
O	Glycosyltransferase (EF_2176)	3.7	29.51/6.36	4	25
S	Pyruvate dehydrogenase complex, PdhB (EF 1354)		35.37/4.61	9	44
X	Triosephosphate isomerase (EF 1962)	3.7	21.12/4.63	6	37
Y	Triosephosphate isomerase (EF 1962)	2.95	21.12/4.63	6	37
Group 3, translation machinery					
D	tRNA uridine modification enzyme GidA (EF 3311)	2.49	69.64/5.72	9	21
H	Elongation factor G (EF_0200)		76.63/4.8	7	20
J	Tyrosyl-*t*-RNA synthetase (EF_0633)	1.96	47.23/5.09	5	21
Group 4, proteases					
P	Zn-metalloprotease, GelE (EF_1818)	1.77	55.34/4.99	5	16
Q	Zn-metalloprotease, GelE (EF_1818)	1.65	55.47/4.99	6	20
R	Zn-metalloprotease, GelE (EF_1818)	1.46	55.34/4.99	15	18

Absence of SalB peptidoglycan hydrolase activity. Muralytic activity of SalB was investigated with six-histidine tag-purified enzyme. Initial analyses used SDS-PAGE renaturing zymograms supplemented with 10 OD units of purified peptidoglycan from *E. faecalis* OG1RF or *M. luteus*. SalB produced unstained zones of clearing on gels after renaturation and methylene blue staining, indicating either murein hydrolytic or peptidoglycan binding capability (data not shown). An assay of peptidoglycan hydrolase activity with purified enzyme and peptidoglycan from strain OG1RF revealed no change in A_{540} after prolonged (up to 24-h) incubation (data not shown). In a separate experiment, reverse phase (RP)-HPLC revealed an absence of soluble muropeptides after over-

TABLE 3 MALDI-TOF MS protein identity assignations

Spot no.	Protein description (accession no.)	Fold change	Calculated mass (kDa)/pI value	No. of peptides matched	Sequence coverage (%)
Group 1, cell division/cell wall synthesis					
2	D-Alanine-D-lactate ligase (EF_2294)	−4.47	21.24/4.7	6	52
7	D-Alanyl-D-alanine carboxypeptidase (Q30BF0_ENTFA)	−2.4	29.4/5.2	9	55
17	Septation ring formation regulator EzrA (EF_0370)	−1.55	68.1/4.8	8	24
5	DnaE protein; DNA Pol III alpha subunit (EF_1044)		31.3/5	5	35
4	DNA primase (EF_1521)	−4.47	73/5.1	6	19
Group 2, miscellaneous					
1	GTP-binding protein LepA (EF_2352)	−2.1	68.3/5	10	20
3	GTP-binding protein LepA (EF_2352)	−4.47	68.3/5	5	16
6	Transcriptional regulator, Cro/CI family (EF_2508)	−8.05	20.9/5.8	4	34

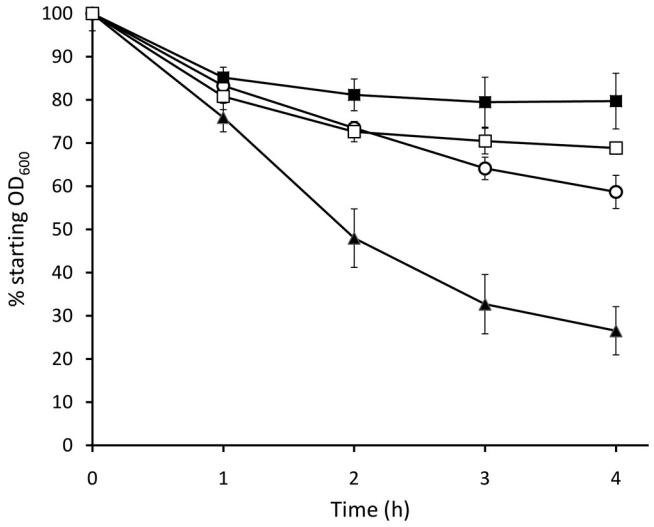

FIG 3 Autolysis of *E. faecalis* strains after addition of penicillin G. Strains are OG1RF (open circles), TX5264 (OG1RF *gelE*) (filled squares), Liv729 (OG1RF *salB*) (filled triangles), and Liv1016 (OG1RF *gelE salB*) (open squares). Error bars represent standard errors of the means from triplicate experiments. Statistically significant differences ($P < 0.05$) in autolysis were determined at 2 h, 3 h, and 4 h for Liv729 relative to OG1RF and for Liv1016 relative to TX5264, using Student's *t* test.

night incubation of SalB with *E. faecalis* OG1RF peptidoglycan (Fig. 7). Moreover, mutanolysin digestion of peptidoglycan isolated from strain OG1RF and strain Liv729 (OG1RF *salB*) revealed identical RP-HPLC traces (Fig. 7 and data not shown).

TABLE 4 FACS viability results

E. faecalis strain	Mean green fluorescence (RU)[a]/fold difference relative to OG1RF	% Dead cells/fold difference relative to OG1RF
TX4002 (OG1RF)	1.80/1	0.37/1
TX5264 (OG1RF *gelE* mutant)	2.60/1.44	2.95/7.97
Liv729 (OG1RF *salB*)	3.30/1.83	14.31/38.67
Liv883 (OG1RF *salB* pAT18::*salB*)	3.06/1.7	4.93/13.32
Liv1016 (OG1RF *gelE salB*)	10.46/5.81	53.91/145.70

[a] RU, relative units.

DISCUSSION

Study of the factors contributing to the culture supernatant protein complement of *E. faecalis* OG1RF identified that a *gelE* metalloprotease mutant produced distinct exoproteins. One prominent protein expressed throughout growth in the mutant was identified as SalB. The enzymatic function of SalB from previous studies is not clear, with its inactivation resulting in defective cell morphology and reduced resistance to various environmental stressors in strain JH2-2 (5). In addition, a *salB* mutant of strain OG1RF is defective for biofilm formation and has increased binding capacity to ECM molecules (17). The link between increased SalB in culture supernatant and *gelE* inactivation identified here was not clear. To investigate the possibility of epistasis between *gelE* and *salB*, a double mutant was generated and the strains were compared by analyzing their exoprotein profile, autolytic activity, cell morphology, and viability.

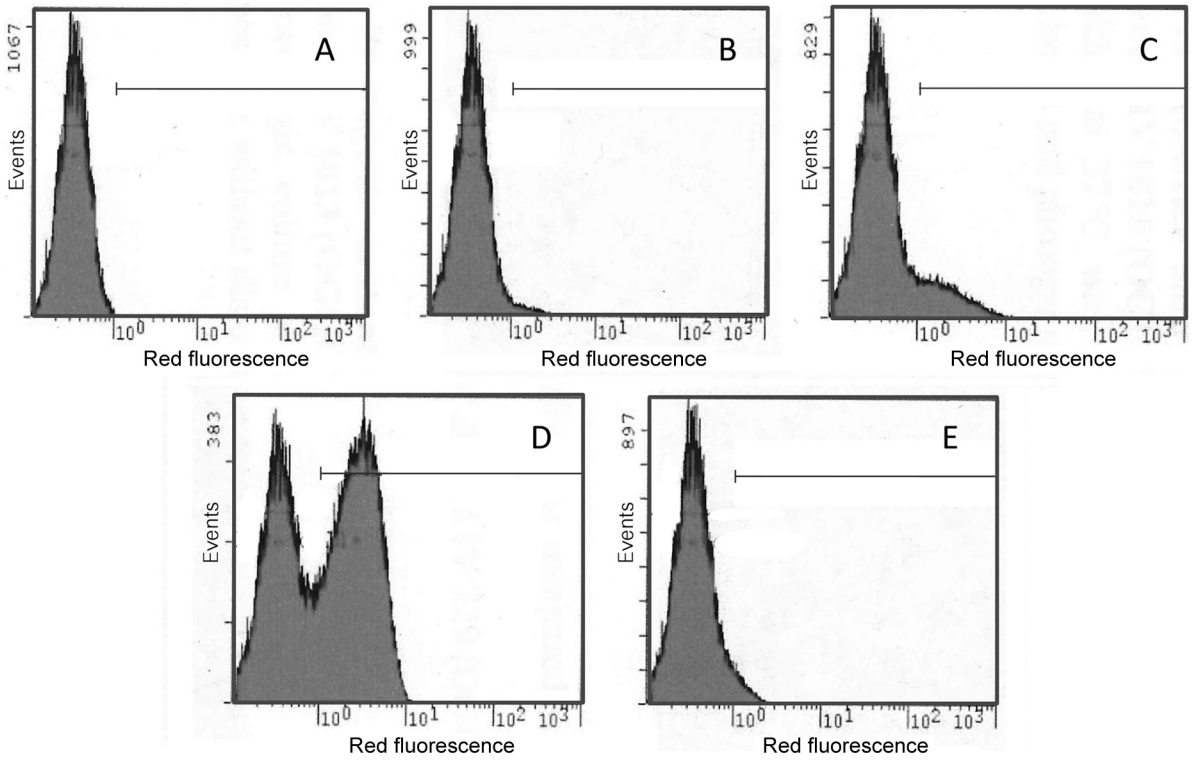

FIG 4 Analysis of viability in cell populations using fluorescence-activated cell sorting (FACS) analysis. Cells were labeled using the Live/Dead viability assay kit (Invitrogen), and 100,000 events were recorded. OG1RF (A), TX5264 (OG1RF *gelE*) (B), Liv729 (OG1RF *salB*) (C), Liv1016 (OG1RF *salB gelE*) (D), and Liv883 (OG1RF *salB* pAT18::*salB*) (E) were harvested at exponential (5 h) growth phase. Horizontal lines mark populations of dead cells.

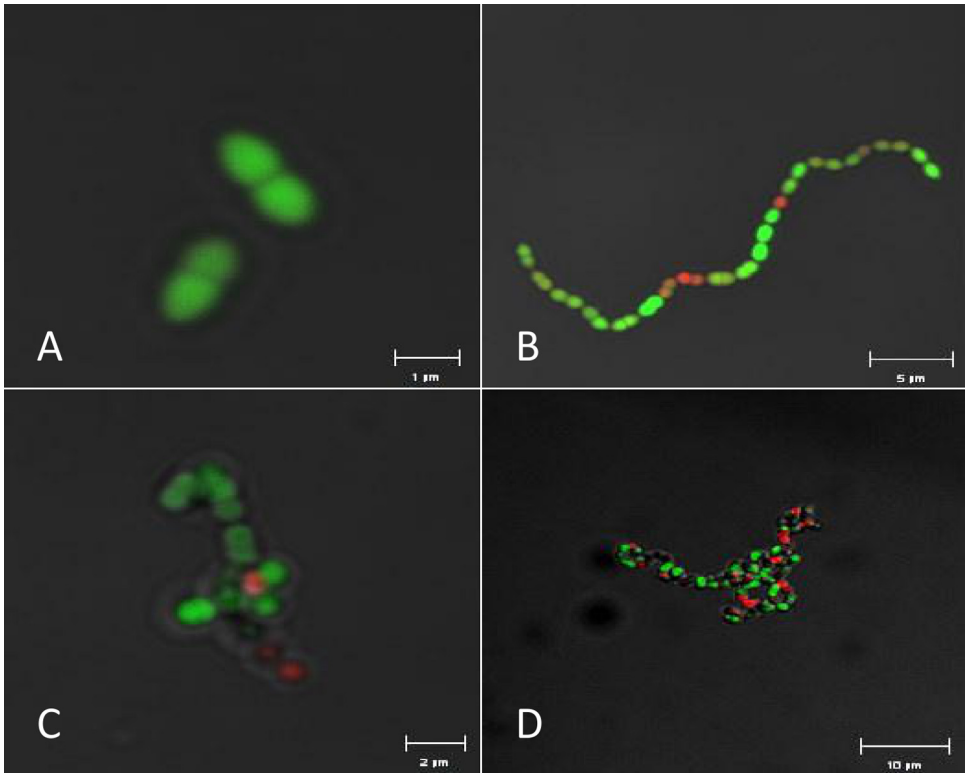

FIG 5 Cell morphology and viability determination of *E. faecalis* strains. Cells of strains TX4002 OG1RF (A), TX5264 (OG1RF *gelE*) (B), Liv729 (OG1RF *salB*) (C), and Liv1016 (OG1RF *gelE salB*) (D) were labeled with BacLight live/dead stain and visualized using laser scanning microscopy. Bars indicate the scales, which vary among the images due to varied morphology (1, 5, 2, and 10 μm, respectively, for panels A, B, C, and D).

Examination of the exoproteins released into culture supernatant by the OG1RF *salB* mutant revealed a complement distinct from the wild type. Consequently, as an attempt to gain further insight into the enzymatic role of SalB, a comparative proteomic study of strain Liv729 (OG1RF *salB*) and the wild-type strain (OG1RF) was undertaken. Relative to its parent, the *salB* mutant released reduced levels of several proteins with ascribed functions in cell wall metabolism and cell replication into culture supernatant. Higher levels were determined for several general stress response proteins (e.g., GroEL, DnaK, and SOD), glycolytic and translation machinery proteins, and GelE (Table 2). The reduced viability of the *salB* mutant indicates that cell lysis might contribute to the exoproteome and could explain the differences with OG1RF. Equally, the identified protein abundance differences could be a consequence of a cellular response to the problems encountered with cell division. The protein complement supports known phenotypes of the *salB* mutant strain; moreover, it potentially defines roles for SalB. Previous studies determined that a *salB* mutant has reduced sensitivity to environmental stress and *salB* transcription is directly regulated by the two-component signal transduction system CroRS (14, 18). The stimulus activating CroRS is unknown. The finding in this study that there are elevated levels of general stress proteins, including DnaK, GroEL, Dps, and SOD, expressed by the *salB* mutant supports the possibility that the *salB* mutant has an inherent stress defect resulting from gene inactivation. The observed concomitant increased level of glycolytic enzymes could indicate a cellular response to membrane dysfunction, with a resulting requirement for direct energy generation via glycolysis. Definitive evidence for a membrane defect has not been obtained; however, there is a clear association between SalB and cell morphology and division septum formation/placement. Induction of stress genes was similarly observed in a *Streptococcus pneumoniae* strain with reduced expression of PcsB (2). It was demonstrated by Le Breton et al. (5, 14) that a *salB* deletion in strain JH2-2 caused morphological defects, which were confirmed in this study for strain OG1RF *salB* using TEM. The double mutant strain Liv1016 (OG1RF *gelE salB*) displayed a higher incidence of irregularities in septum formation, including multiple septa, than strain Liv729 (OG1RF *salB*). Thus, the absence of GelE exacerbates the phenotype described for *salB* inactivation, although there is not clear evidence that this is due directly to GelE proteolysis of SalB. The high level of GelE in the supernatant of the *salB* mutant (Table 2) compared to that of strain OG1RF suggests a compensatory aspect to the expression levels of these proteins. A *Streptococcus agalactiae* mutant of PcsB (SalB homologue) produces cell aggregation similar to that of an *E. faecalis salB* mutant (23, 24). The role of PcsB has been studied in several streptococci, in which the location of *pcsB*, immediately downstream of the cell shape-determining operon *mreCD*, is conserved, similar to the location of *salA*, the *E. faecalis* homologue of *salB* and *pcsB*. The reduced level of the cell division protein EzrA in culture supernatant of the OG1RF *salB* mutant lends further support to a theoretical role for SalB in cell division and/or cell shape determination.

The incorrect septum placement in the *E. faecalis* OG1RF *salB* mutant is likely to alter the plane of division to produce the cell

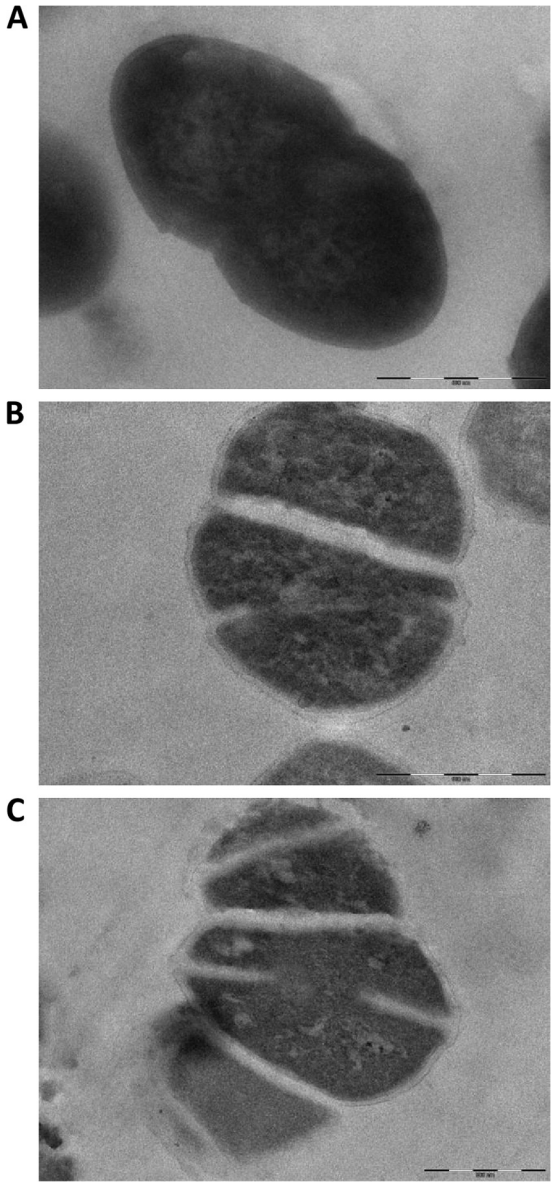

FIG 6 Transmission electron microscopy of thin sections of mid-exponentially growing cells of strains TX5244 (OG1RF) (A), Liv729 (OG1RF *salB*) (B), and Liv1016 (OG1RF *gelE salB*) (C). Scale bar, 500 nm.

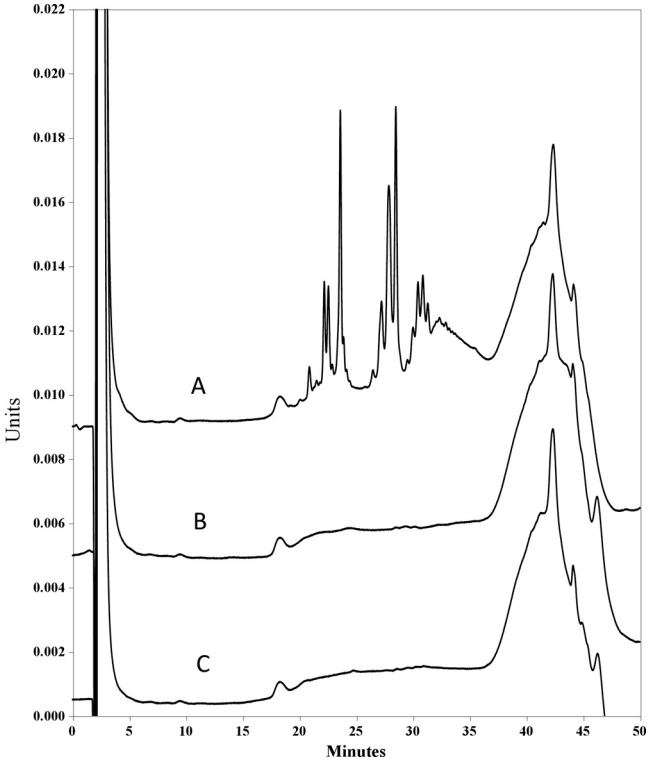

FIG 7 Separation of soluble muropeptides by HPLC after incubation with enzymes. OG1RF peptidoglycan was incubated overnight with 5 μg of mutanolysin (Sigma) (A) or 50 μg of SalB (B) or without enzyme (control) (C).

clumps in the single and multiple mutants studied here. It is tempting to speculate that since GelE regulates the activity of the major cell wall autolysins of *E. faecalis* OG1RF, the exacerbated phenotype observed in strain Liv1016 (OG1RF *gelE salB*) supports the linking of SalB to cell division, in part determining the characteristic ovococcal morphology. Certainly, the morphology of a *salB* mutant and that of a *divIVA* (*trans* complementation) mutant of *E. faecalis* are strikingly similar (22). The modulation of SalB expression by the CroRS two-component signal transduction regulator links cell morphology with intrinsic β-lactam resistance (7, 18). Recent analysis of PcsB in *S. pneumoniae* has provided the first evidence supporting a role for PcsB/SalB/SagA family proteins in the cell division complex via its interaction with FtsX (28).

An unexpected finding from laser scanning microscopy and flow cytometry of viability stained cells of strain Liv729 (OG1RF *salB*) was the proportion of red-fluorescent dead cells (14.31%) present in the population compared with OG1RF red-fluorescent dead cells (0.37%) (Table 4). This proportion was greatly increased in strain Liv1016 (OG1RF *salB gelE*) (53.9%). These measurements do not take account of the fact that changes in cell volume would increase uptake of stain in the mutants, since cell volumes were not measured in this study. The corresponding changes in green fluorescence, however, identify that although there were more cells per event due to defective cell separation in the *salB* mutants, the relative levels of red (dead) cells were disproportionately high. Complementation of the *salB* mutant via strain Liv883 (OG1RF *salB* pAT18::*salB*) only partially rescued this phenotype.

Previous studies hypothesized that SalB and its homologues might possess peptidoglycan hydrolase activity. Cell autolysis and activity assays of the purified SalB were performed to investigate its function further. In an autolysis assay, a strain under penicillin challenge, Liv729 (OG1RF *salB*), displayed greater levels of lysis than the wild type. As expected, the absence of GelE in strain TX5264 (OG1RF *gelE*) resulted in decreased autolysis compared with the wild type (Fig. 3). Similarly, reduced autolysis was observed in the presence of Triton X-100 with strain TX5264 (OG1RF *gelE*), while strain Liv729 (OG1RF *salB*) again showed significantly enhanced autolysis. Complementation restored wild-type autolysis rates to strain Liv883 (OG1RF *salB* pAT18::*salB*) under penicillin challenge, but not under Triton X-100 challenge (data not shown). Peptidoglycan hydrolysis was tested using both zymograms and HPLC of either muramidase-digested pep-

tidoglycans or wild-type peptidoglycan incubated with purified SalB. Renaturing zymograms performed with an SDS-PAGE gel supplemented with purified peptidoglycan from *E. faecalis* OG1RF or *Micrococcus luteus* ATCC 4698 revealed clearing. Since this could indicate either peptidoglycan binding by SalB preventing methylene blue staining or peptidoglycan hydrolysis, the activity of purified peptidoglycan was tested with six-histidine-tagged SalB at a range of pH values in different buffers with several divalent cations. However, no detectable activity was observed by using this assay (data not shown). Moreover, the peptidoglycans from Liv729 (OG1RF *salB*) and OG1RF were indistinguishable upon mutanolysin digestion and separation by HPLC, indicating that the clearing observed on the zymograms most likely represented peptidoglycan binding by SalB (Fig. 7 and data not shown). A lack of *in vitro* peptidoglycan hydrolysis was reported for PcsB of *S. agalactiae* and *S. pneumoniae* (9, 23, 24). Very recently, evidence was obtained supporting a role for PcsB interacting with the FtsX cell division protein and supporting a potential role for direct or indirect PG hydrolysis during cell division (28).

While the data presented here do not determine the cellular role for SalB or support peptidoglycan hydrolysis activity, the findings are certainly consistent with SalB having a role in cell shape determination and/or cell division. The septation anomalies and the reduced level of EzrA in the *salB* mutant culture supernatant exoprotein profile relative to the wild type could result from direct interaction of SalB with a cell division protein, in which the coiled-coil domain located in the N-terminal region of SalB has the potential to mediate this interaction.

ACKNOWLEDGMENTS

This research was supported by BBSRC postgraduate award BB/S/K/2004/11198 to R.G.W. and a Dorothy Hodgkin NERC-BP postgraduate award to J.S.

We thank Barbara Murray for kindly providing strains and plasmids that were essential for parts of this study. We are grateful for bioinformatic assistance from Daniel Rigden.

REFERENCES

1. **Arias CA, Cortes L, Murray BE.** 2007. Chaining in enterococci revisited: correlation between chain length and gelatinase phenotype, and *gelE* and *fsrB* genes among clinical isolates of *Enterococcus faecalis*. J. Med. Microbiol. **56**:286–288.
2. **Barendt SM, et al.** 2009. Influences of capsule on cell shape and chain formation of wild-type and *pcsB* mutants of serotype 2 *Streptococcus pneumoniae*. J. Bacteriol. **191**:3024–3040.
3. **Biavasco F, et al.** 1996. In vitro conjugative transfer of VanA vancomycin resistance between enterococci and listeriae of different species. Eur. J. Clin. Microbiol. Infect. Dis. **15**:50–59.
4. **Bonten MJ, Willems R, Weinstein RA.** 2001. Vancomycin-resistant enterococci: why are they here and where do they come from? Lancet Infect. Dis. **1**:314–325.
5. **Breton YL, et al.** 2002. Isolation and characterization of bile salts-sensitive mutants of *Enterococcus faecalis*. Curr. Microbiol. **45**:434–439.
6. **Chaussee MA, McDowell EJ, Chaussee MS.** 2008. Proteomic analysis of proteins secreted by *Streptococcus pyogenes*. Methods Mol. Biol. **431**:15–24.
7. **Comenge Y, et al.** 2003. The CroRS two-component regulatory system is required for intrinsic beta-lactam resistance in *Enterococcus faecalis*. J. Bacteriol. **185**:7184–7192.
8. **Eckert C, Lecerf M, Dubost L, Arthur M, Mesnage S.** 2006. Functional analysis of AtlA, the major N-acetylglucosaminidase of *Enterococcus faecalis*. J. Bacteriol. **188**:8513–8519.
9. **Giefing-Kroll C, Jelencsics KE, Reipert S, Nagy E.** 2011. Absence of pneumococcal PcsB is associated with overexpression of LysM domain-containing proteins. Microbiology **157**:1897–1909.
10. **Gilmore MS, Ferretti JJ.** 2003. The thin line between gut commensal and pathogen. Science **299**:1999–2002.
11. **Hancock LE, Gilmore MS.** 2006. Pathogenicity of enterococci, p 301–354. *In* Fischetti V, Novick R, Ferretti J, Portnoy D, Rood J (ed), Gram-positive organisms. ASM Press, Washington, DC.
12. **Horsburgh MJ, Wiltshire MD, Crossley H, Ingham E, Foster SJ.** 2004. PheP, a putative amino acid permease of *Staphylococcus aureus*, contributes to survival in vivo and during starvation. Infect. Immun. **72**:3073–3076.
13. **Land AD, Winkler ME.** 2011. The requirement for pneumococcal MreC and MreD is relieved by inactivation of the gene encoding PBP1a. J. Bacteriol. **193**:4166–4179.
14. **Le Breton Y, et al.** 2003. Molecular characterization of *Enterococcus faecalis* two-component signal transduction pathways related to environmental stresses. Environ. Microbiol. **5**:329–337.
15. **Mesnage S, Chau F, Dubost L, Arthur M.** 2008. Role of N-acetylglucosaminidase and N-acetylmuramidase activities in *Enterococcus faecalis* peptidoglycan metabolism. J. Biol. Chem. **283**:19845–19853.
16. **Miller D, Urdaneta V, Weltman A.** 2002. Public health dispatch: vancomycin-resistant *Staphylococcus aureus*—Pennsylvania. MMWR Morb. Mortal. Wkly. Rep. **51**:902.
17. **Mohamed JA, Teng F, Nallapareddy SR, Murray BE.** 2006. Pleiotrophic effects of 2 *Enterococcus faecalis sagA*-like genes, *salA* and *salB*, which encode proteins that are antigenic during human infection, on biofilm formation and binding to collagen type I and fibronectin. J. Infect. Dis. **193**:231–240.
18. **Muller C, et al.** 2006. The response regulator CroR modulates expression of the secreted stress-induced SalB protein in *Enterococcus faecalis*. J. Bacteriol. **188**:2636–2645.
19. **Nakayama J, Kariyama R, Kumon H.** 2002. Description of a 23.9-kilobase chromosomal deletion containing a region encoding fsr genes which mainly determines the gelatinase-negative phenotype of clinical isolates of *Enterococcus faecalis* in urine. Appl. Environ. Microbiol. **68**:3152–3155.
20. **Paulsen IT, et al.** 2003. Role of mobile DNA in the evolution of vancomycin-resistant *Enterococcus faecalis*. Science **299**:2071–2074.
21. **Qin X, Singh KV, Weinstock GM, Murray BE.** 2001. Characterization of *fsr*, a regulator controlling expression of gelatinase and serine protease in *Enterococcus faecalis* OG1RF. J. Bacteriol. **183**:3372–3382.
22. **Ramirez-Arcos S, Liao M, Marthaler S, Rigden M, Dillon JA.** 2005. *Enterococcus faecalis divIVA*: an essential gene involved in cell division, cell growth and chromosome segregation. Microbiology **151**:1381–1393.
23. **Reinscheid DJ, Ehlert K, Chhatwal GS, Eikmanns BJ.** 2003. Functional analysis of a PcsB-deficient mutant of group B *Streptococcus*. FEMS Microbiol. Lett. **221**:73–79.
24. **Reinscheid DJ, Gottschalk B, Schubert A, Eikmanns BJ, Chhatwal GS.** 2001. Identification and molecular analysis of PcsB, a protein required for cell wall separation of group B *Streptococcus*. J. Bacteriol. **183**:1175–1183.
25. **Rince A, et al.** 2003. Physiological and molecular aspects of bile salt response in *Enterococcus faecalis*. Int. J. Food Microbiol. **88**:207–213.
26. **Rosenthal RS, Dziarski R.** 1994. Isolation of peptidoglycan and soluble peptidoglycan fragments. Methods Enzymol. **235**:253–285.
27. **Seno Y, Kariyama R, Mitsuhata R, Monden K, Kumon H.** 2005. Clinical implications of biofilm formation by *Enterococcus faecalis* in the urinary tract. Acta Med. Okayama **59**:79–87.
28. **Sham LT, Barendt SM, Kopecky KE, Winkler ME.** 2011. Essential PcsB putative peptidoglycan hydrolase interacts with the essential FtsXSpn cell division protein in *Streptococcus pneumoniae* D39. Proc. Natl. Acad. Sci. U. S. A. **108**:E1061–E1069.
29. **Shankar J, Walker RG, Ward D, Horsburgh MJ.** 2012. The *Enterococcus faecalis* exoproteome: identification and temporal regulation by Fsr. PLoS One **7**:e33450. doi:10.1371/journal.pone.0033450.
30. **Sievert D, et al.** 2002. *Staphylococcus aureus* resistant to vancomycin—United States. MMWR Morb. Mortal. Wkly. Rep. **51**:565–567.
31. **Singh KV, Qin X, Weinstock GM, Murray BE.** 1998. Generation and testing of mutants of *Enterococcus faecalis* in a mouse peritonitis model. J. Infect. Dis. **178**:1416–1420.
32. **Smith TJ, Foster SJ.** 1995. Characterization of the involvement of two compensatory autolysins in mother cell lysis during sporulation of *Bacillus subtilis* 168. J. Bacteriol. **177**:3855–3862.
33. **Tendolkar P, Baghdayan A, Shankar N.** 2003. Pathogenic entero-

cocci: new developments in the 21st century. Cell. Mol. Life Sci. **60**: 2622–2636.
34. **Teng F, Kawalec M, Weinstock GM, Hryniewicz W, Murray BE.** 2003. An *Enterococcus faecium* secreted antigen, SagA, exhibits broad-spectrum binding to extracellular matrix proteins and appears essential for *E. faecium* growth. Infect. Immun. **71**:5033–5041.
35. **Thomas VC, et al.** 2009. A fratricidal mechanism is responsible for eDNA release and contributes to biofilm development of *Enterococcus faecalis*. Mol. Microbiol. **72**:1022–1036.
36. **Trieu-Cuot P, Carlier C, Poyart-Salmeron C, Courvalin P.** 1991. Shuttle vectors containing a multiple cloning site and a *lacZ* alpha gene for conjugal transfer of DNA from *Escherichia coli* to Gram-positive bacteria. Gene **102**:99–104.
37. **Waters CM, Antiporta MH, Murray BE, Dunny GM.** 2003. Role of the *Enterococcus faecalis* GelE protease in determination of cellular chain length, supernatant pheromone levels, and degradation of fibrin and misfolded surface proteins. J. Bacteriol. **185**:3613–3623.
38. **Yasmin A, et al.** 2010. Comparative genomics and transduction potential of *Enterococcus faecalis* temperate bacteriophages. J. Bacteriol. **192**:1122–1130.